INSTITUTE OF PHYSICS PUBLISHING JOURNAL OF PHYSICS D: APPLIED PHYSICS

J. Phys. D: Appl. Phys. **40** (2007) 260–265 doi:10.1088/0022-3727/40/1/024

Three-dimensional effect on the effective thermal conductivity of porous media

Moran Wang[1], Jinku Wang[2], Ning Pan[1], Shiyi Chen[3] and Jihuan He[4]

[1] Department of Biological and Agricultural Engineering, University of California, Davis, CA 95616, USA
[2] School of Aerospace, Tsinghua University, Beijing 100084, People's Republic of China
[3] Department of Mechanical Engineering, Johns Hopkins University, Baltimore, MD 21218, USA
[4] College of Science, Donghua University, Shanghai 200051, People's Republic of China

E-mail: mmwang@ucdavis.edu

Received 6 September 2006, in final form 20 October 2006
Published 15 December 2006
Online at stacks.iop.org/JPhysD/40/260

Abstract
A three-dimensional mesoscopic method is developed for predicting the effective thermal conductivity of multiphase random porous media. The energy transport equations are solved by a lattice Boltzmann method for multiphase conjugate heat transfer through a porous structure whose morphology is characterized by a random generation-growth algorithm. Our numerical results show that the cell number in the *third* dimension influences the resulting effective thermal conductivity of three-dimensional porous media. The predicted effective thermal conductivity varies with the cell number in the *third* dimension following an exponential relationship, and it requires in the examples at least 10 cells along the *third* dimension before the predictions stabilize. Comparisons with the experimental data show that the effective thermal conductivities measured by the hot-probe and hot-wire techniques agree well with the predicted results by the two-dimensional model, whereas those measured by the transient comparative method agree more with the three-dimensional predictions.

1. Introduction

For better understanding of transport mechanism in soils, rocks and other engineering materials, the effective thermal conductivity of porous media has been studied for well over one hundred years in both theory and experiment [1–3]. Recently, it has gained more attention due to its new applications in functional material design, MEMS devices cooling techniques, textile and food engineering and even human medical technologies [4–7].

In experiments, the hot-wire and hot-probe are the most popular techniques for local thermal conductivity measurement for *soft* matter, which are based on a linear heat source and an axis-symmetric measurement system [8,9]. They have been used for measuring the thermal conductivities of soils, foods and even liquids [10–17]. In high porosity *solid* structure cases, however, the parallel plate and hot plate have been more frequently used [18–22]. Recently, Carson *et al* [23] developed a 'comparative method' to measure the thermal conductivity in highly non-homogeneous cases.

To model the effective thermal conductivity of porous media, the semi-empirical theoretical models often used are generally based on network combinations of the series and parallel models [24–29]. Wang *et al* [30] also presented simple combinatory rules for complex materials. Owing to the rapid developments in computer and computational techniques in the past twenty years, pure numerical modelling methods have been used to predict the thermal conductivity of porous media [31–43]. Thovert *et al* [31] calculated the thermal conductivity of random media and regular fractals by solving the Laplace equation using the finite-difference method. Bakker [32] determined the thermal conductivity of porous media through the finite element method. However,

the traditional partial difference equation (PDE) solvers often impose huge or even prohibitive computational cost when the porous structure is too complicated, especially when the fluid–solid conjugate problem is considered. Therefore the stochastic–statistic methods for transport in porous media have gained increasing attention in recent years [33, 34]. Shoshany *et al* [35] and Barta and Dieska [36] modelled the thermal conductivity of porous materials using the Monte Carlo methods. Zhang *et al* [37, 38] developed a randomly mixed model (RMM) to predict the effective thermal conductivity of moist porous media. However, Qian *et al* [39] used a two-dimensional five-speed (D2Q5) lattice Boltzmann model to simulate the effective thermal conductivity of porous materials with no fluid–solid conjugate heat transfer considered. Wang *et al* [40] built up a full stochastic–statistic approach for the effective thermal conductivity predictions of random porous media, which include a two-dimensional nine-speed (D2Q9) lattice Boltzmann method (LBM) for fluid–solid conjugate heat transfer [41] and a random generation-growth method to generate morphology of multiphase random porous media. Wang's predictions agreed rather well with a series of experimental data.

Based on the previous work, this paper will develop a three-dimensional stochastic–statistic based method for predicting the effective thermal conductivity of porous media. The results will be compared with the two-dimensional predictions and the existing experimental data. The three-dimensional effect of the effective thermal conductivity of porous media will therefore be discussed.

2. Numerical method

2.1. Lattice Boltzmann algorithm

The LBM is intrinsically a mesoscopic approach based on the evolution of statistical distribution on lattices and has achieved considerable success in simulating fluid flows and associated transport phenomena [42–44]. The most important advantages of the LBM are the easy implementation of multiple intercomponent interactions and complex geometry boundary conditions [45, 46]. Conservations can hold automatically in general without additional computational efforts [47, 48]. The thermal models for the two-dimensional and three-dimensional LBM have been developed recently [49–51]. Here we have adapted our previous lattice Boltzmann algorithm for fluid–solid conjugate heat transfer [41] into the three-dimensional mode.

For the pure thermal conduction in porous media, the temperature evolution equation in either the fluid or the solid phase can be generally given as

$$g_\alpha(\boldsymbol{r}+\boldsymbol{e}_\alpha\delta_t, t+\delta_t) - g_\alpha(\boldsymbol{r}, t) = -\frac{1}{\tau_g}[g_\alpha(\boldsymbol{r}, t) - g_\alpha^{\mathrm{eq}}(\boldsymbol{r}, t)], \tag{1}$$

where g_α^{eq} is the equilibrium distribution in each direction, $\boldsymbol{e}_\alpha$ the discrete lattice velocity and τ_g the dimensionless relaxation time for each phase. For a D2Q9 model, they are

$$g_\alpha^{\mathrm{eq}} = \begin{cases} 0 & \alpha = 0 \\ \frac{1}{6}T & \alpha = 1 \text{ to } 4 \\ \frac{1}{12}T & \alpha = 5 \text{ to } 8, \end{cases} \tag{2}$$

$$\boldsymbol{e}_\alpha = \begin{cases} (0, 0) & \alpha = 0 \\ (\pm1, 0)c, (0, \pm1)c & \alpha = 1 \text{ to } 4 \\ (\pm1, \pm1)c & \alpha = 5 \text{ to } 8 \end{cases} \tag{3}$$

and

$$\tau_g = \frac{3}{2}\frac{k}{c^2\delta_t} + 0.5, \tag{4}$$

while for a D3Q15 model they are

$$g_\alpha^{\mathrm{eq}} = \begin{cases} 0 & \alpha = 0 \\ \frac{1}{9}T & \alpha = 1 \text{ to } 6 \\ \frac{1}{24}T & \alpha = 7 \text{ to } 14, \end{cases} \tag{5}$$

$$\boldsymbol{e}_\alpha = \begin{cases} (0, 0, 0) & \alpha = 0 \\ (\pm1, 0, 0)c, (0, \pm1, 0)c, (0, 0, \pm1)c & \alpha = 1 \text{ to } 6 \\ (\pm1, \pm1, \pm1)c & \alpha = 7 \text{ to } 14, \end{cases} \tag{6}$$

and

$$\tau_g = \frac{9}{5}\frac{k}{c^2\delta_t} + 0.5, \tag{7}$$

where δ_t is the time step, k the thermal conductivity for each phase and c a *pseudo* sound speed whose value can take any positive value theoretically only to insure the τ_g value within (0.5, 2) [41, 46]. The temperature and the heat flux can then be calculated according to [52]

$$T = \sum_\alpha g_\alpha, \tag{8}$$

$$q = \left(\sum_\alpha \boldsymbol{e}_\alpha g_\alpha\right)\frac{\tau_g - 0.5}{\tau_g}. \tag{9}$$

After the temperature field is solved, the effective thermal conductivity, k_{eff}, can be determined:

$$k_{\mathrm{eff}} = \frac{L \cdot \int q \cdot \mathrm{d}A}{\Delta T \int \mathrm{d}A}, \tag{10}$$

where q is the steady heat flux through the media cross section area $\mathrm{d}A$ between the temperature difference ΔT with a distance L.

2.2. Boundary conditions

For the isothermal boundary treatment, we follow the bounce-back rule of the non-equilibrium distribution proposed by Zou and He [53]:

$$g_\alpha - g_\alpha^{\mathrm{eq}} = -(g_\beta - g_\beta^{\mathrm{eq}}), \tag{11}$$

where α and β represent opposite directions, and the equilibrium distribution can be calculated based on the local boundary temperature.

Table 1. Predictions of effective thermal conductivities for two kinds of structures.

	Parallel mode		Series mode	
Results c(m s^{-1})	Predictions (W m^{-1}K^{-1})	Deviations (%)	Predictions (W m^{-1}K^{-1})	Deviations (%)
100	1.262 674 91	0.0139	0.049 504 95	0.0000
1 000	1.262 448 15	−0.0058	0.049 504 95	0.0000
10 000	1.262 566 10	0.0052	0.049 504 95	0.0000

where $k_1 = 2.5$ W m^{-1} K^{-1}, $k_2 = 0.025$ W m^{-1} K^{-1}.

For the insulated boundary, we tried the Neumann boundary treatment [41, 52] and let the boundary temperature gradient be equal to zero. To prevent heat flux from leaking along the insulate surfaces, a specular reflection treatment is implemented. It has been proved that the current boundary treatments have the second order accuracies [53].

3. Results and discussion

The proposed method will be used to predict the effective thermal conductivity of the three-dimensional porous media in this section. First of all, the method is validated by comparing with the theoretical solutions for two simple structures. The three-dimensional predictions with proper simulation parameters will then be compared against the two-dimensional cases and experimental data so that the *third* dimension influence on the effective thermal conductivity of porous media is discussed.

3.1. Benchmarks

To validate the algorithm and the codes, the numerical predictions are compared with the theoretical solutions for two hypothetical structure cases: parallel mode and series mode. The structures are formed in two phases and the thermal conductivities are 2.5 W m^{-1}K^{-1} and 0.025 W m^{-1}K^{-1}, respectively. The fractions of the two phases are equal so that the theoretical solution of the effective thermal conductivity is 1.2625 W m^{-1}K^{-1} for parallel mode and 0.049 504 95 W m^{-1}K^{-1} for series mode. Table 1 lists our predictions of the effective thermal conductivities and the deviations from the simple theoretical solutions as functions of the pseudo sound speed c. It is clear that our predictions agree perfectly well with the theoretical solutions with the maximum deviation less than 0.02% when c changes from 100 to 10000 m s^{-1}. The results validate the proposed algorithm and the boundary implements. A larger c leads to a more accurate prediction yet requires a higher computational cost. In the following simulations, c is set to 1000 m s^{-1} unless specified otherwise.

3.2. Randomly generated porous media

To bring the random characteristics of natural porous media into modelling, the random effect has to be introduced during the generation of porous media structure. The random location of obstacles is the most popular method to construct an artificial porous medium [35–38]. Coveney *et al* [54] proposed a pore growth-with-time model to control the pores size and connectivity. Wang *et al* [40] presented a full description of the structure generation method, termed the quartet structure generation set (QSGS), for generating micro-morphology of random porous media based on the cluster growth theory [55]. The QSGS method has been used in two-dimensional simulations and has shown good agreement with a series of experimental data. Here we implement the QSGS method in three-dimensional isotropic systems.

Table 2. Predicted effective thermal conductivities for different core distribution probabilities.

c_d	k_{eff}(W m^{-1}K^{-1})	$k_{eff}/k_{eff,c_d=0.3}$
0.001	1.501	0.9311
0.01	1.519	0.9423
0.1	1.592	0.9876
0.3	1.612	1.0000

where $k_s = 2.50$ W m^{-1} K^{-1}, $k_g = 0.025$ W m^{-1} K^{-1}.

To distinguish the present QSGS method from the previous random obstacle location method [38], the effect of core distribution probability, c_d, on the effective thermal conductivity is studied. Consider the gas–solid porous media at a porosity $\varepsilon = 0.7$. The solid cores grow by the QSGS method with a fraction of 0.3. When c_d equals 0.3, the QSGS method will become equivalent to the random obstacle location method. Once c_d is smaller than 0.3, each solid core will have a three-dimensional structure, not just a cube.

Table 2 shows our predicted effective thermal conductivities versus the core distribution probability, c_d, at $k_s = 2.50$ W m^{-1}K^{-1} and $k_g = 0.025$ W m^{-1}K^{-1}. The results reveal that the effective thermal conductivity of porous media decreases with the core distribution probability. When c_d changes from 0.3 to 0.01, the effective thermal conductivity decreases by over 5%. It is indicated that the influence of porous structures on the effective thermal conductivity should be taken into consideration if the pore size is not negligible.

3.3. Influence of the third dimension

The three-dimensional transport phenomena often differ from the two-dimensional cases under the same boundary conditions due to the different surface-to-volume ratio [56, 57]. Wang and Li [58] compared the gas flows in two- and three-dimensional microchannels and found an exponential relationship between the velocities in a three-dimensional channel and in a two-dimensional channel. Here we perform the effective thermal conductivity predictions in both two- and three-dimensions under the same boundary conditions and with the same simulation parameters. We maintain the identical length and height of the 2D cell domains but add the cell number along the *third* dimension to set up a 3D case. Comparisons between the three-dimensional results for different cell numbers in the

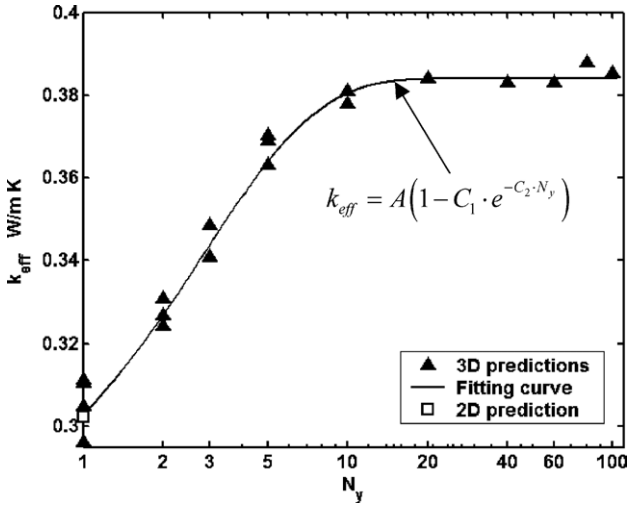

Figure 1. The predicted effective thermal conductivities of three-dimensional two-phase porous media versus the cell numbers N_y in the *third* direction. The simulation parameters are $k_s = 0.60\,\mathrm{W\,m^{-1}\,K^{-1}}$, $k_g = 0.035\,\mathrm{W\,m^{-1}\,K^{-1}}$, $\varepsilon = 0.3$ and $c_\mathrm{d} = 0.01$. The fitted parameters are $A = 0.384$, $C_1 = 0.30$ and $C_2 = 0.35$.

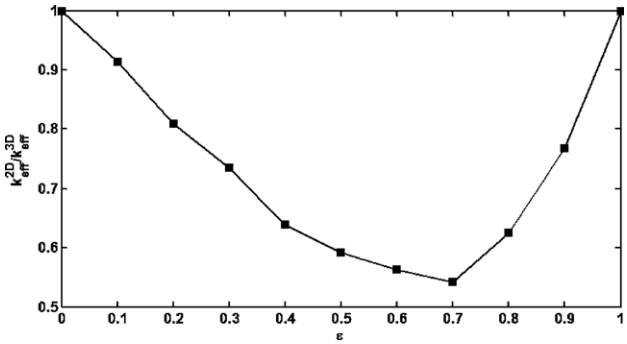

Figure 2. The ratios of two-dimensional to three-dimensional predicted effective thermal conductivities for different porosities of three-dimensional two-phase porous media. The simulation parameters are $k_s = 0.60\,\mathrm{W\,m^{-1}\,K^{-1}}$, $k_g = 0.035\,\mathrm{W\,m^{-1}\,K^{-1}}$ and $c_\mathrm{d} = 0.01$.

third dimension and the two-dimensional results will indicate the three-dimensional effects.

The two-phase porous media are generated at $\varepsilon = 0.3$, $c_\mathrm{d} = 0.01$ and the simulation parameters are $k_s = 0.60\,\mathrm{W\,m^{-1}K^{-1}}$ and $k_g = 0.035\,\mathrm{W\,m^{-1}K^{-1}}$. The grids for the two-dimensional predictions are set as $N_2 \times N_2$, where $N_2 = 200$, and for the three-dimensional predictions as $N_3 \times N_y \times N_3$, where a typical value of N_3 is normally 200. We have changed the values of N_3 from 60 to 300, and the results remain almost the same. For the current grid arrangements, the discretization errors are smaller than 3% caused by the random structures.

Figure 1 shows the impact of the *third* dimension cell numbers N_y on the effective thermal conductivity predictions. The two-dimensional result is plotted in the same figure, which can be viewed as a special case of the three-dimensional result at $N_y = 1$. The three-dimensional effective thermal conductivity increases sharply with the *third* dimension cell number when $N_y < 10$ and then levels off for larger N_y. Similar to [58], a similar exponential relationship is obtained by fitting the predictions as shown in figure 1. For the specific simulation case, the fitted parameters are $A = 0.384$, $C_1 = 0.30$, $C_2 = 0.35$.

The results indicate the following: (i) the predicted effective thermal conductivities are always smaller at two-dimensional cases than at three-dimensional ones under the same boundary conditions and simulation parameters, which is consistent with the previous work of Kirkpatrick based on the effective medium theory [59], (ii) the cell number in the *third* dimension has to be at least over a certain number (=10 in this case) to stabilize the influence of the third dimension and (iii) once the cell number in the third dimension is large enough, the predicted effective thermal conductivity becomes independent of the cell number N_y.

Furthermore, the ratios of the predicted effective thermal conductivities between 2D and 3D are also related to the porosities. Figure 2 depicts the relationship by using the simulation parameters as $k_s = 0.60\,\mathrm{W\,m^{-1}K^{-1}}$, $k_g = 0.035\,\mathrm{W\,m^{-1}K^{-1}}$ and $c_\mathrm{d} = 0.01$. The results indicate again that the two-dimensional predictions are always smaller than the three-dimensional ones unless the porosity ε equals zero or unity. The ratio does not vary with the porosity monotonically and reaches a minimum value, in this case, smaller than 0.6 when the porosity $\varepsilon \approx 0.7$.

3.4. Comparisons with experimental data

The present two- and three-dimensional predictions are also compared with the existing experimental data. As reviewed in the introduction, the hot-probe is a convenient measurement for the effective thermal conductivity in soft matter; however since it is based on a line heat source and axial symmetric assumption, this method is generally regarded as a two-dimensional technique [60]. Wang *et al* [40] have shown that a series of experimental data measured by the hot-probe or hot-wire methods agree well with their two-dimensional predictions. Here we compare the measured effective thermal conductivities of moist sands under frozen and unfrozen states [11, 12] with the corresponding predictions in figure 3. The parameters in both two- and three-dimensional calculations are $\varepsilon = 0.52$, $k_s = 2.85\,\mathrm{W\,m^{-1}K^{-1}}$, $k_w = 0.5924\,\mathrm{W\,m^{-1}K^{-1}}$, $k_g = 0.0249\,\mathrm{W\,m^{-1}K^{-1}}$ and $k_\mathrm{ice} = 2.38\,\mathrm{W\,m^{-1}K^{-1}}$ adopted from [61]. The two-dimensional simulations use a 200×200 grid, and the three-dimensional cases use a $60 \times 60 \times 60$ grid for acceptable computational costs. The results show that the experiment data are consistent with the two-dimensional predictions and yet deviate much from the three-dimensional predictions.

We also notice that Zhang's recent three-dimensional random simulations also exhibit good agreement with the experimental data used [38]. Based on the analysis above, the reason for such agreement might be as follows: (i) the cell number in the third dimension is not large enough so that the three-dimensional simulations are actually close to the two-dimensional ones and (ii) the RMM did not consider the influence of the pore structure, which was actually a special case at $c_\mathrm{d} = \varepsilon$.

Carson *et al* [23] developed a transient comparative method to measure the effective thermal conductivity of a pseudo-porous food analogue. There was no two-dimensional

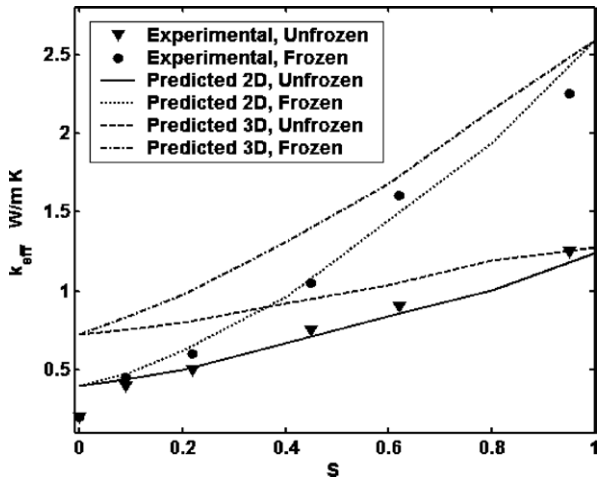

Figure 3. Comparisons between our numerical predictions with the experimental data of Singh *et al* [12] measured by the hot-probe method.

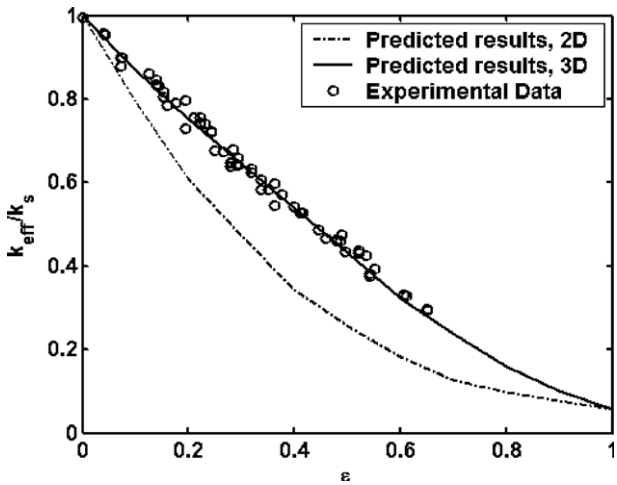

Figure 4. Comparisons between our numerical predictions and the experimental data of Carson *et al* [23] measured by a transient comparative method.

assumption in this measurement technique. Figure 4 shows the comparison of experimental data with the respective two-dimensional and three-dimensional predictions using the present models. The used parameters are $c_d = 0.01$, $k_s = 0.60\,\mathrm{W\,m^{-1}K^{-1}}$ and $k_g = 0.035\,\mathrm{W\,m^{-1}K^{-1}}$. Again the two-dimensional simulations use 200×200 grids and the three-dimensional cases use $60 \times 60 \times 60$ grids. This time, however, the three-dimensional predictions are closer to the experimental data, while the two-dimensional predictions are much lower. Although the generated random structures are not exactly the same as those in Carson's experiments, which might lead to possible differences [62], this comparison may still serve as evidence to show that Carson's transient comparative method is a three-dimensional measurement technique.

4. Conclusions

The three-dimensional effect on the effective thermal conductivity predictions of porous media has been investigated numerically using a stochastic–statistic based method. Compared with the two-dimensional results under the same boundary conditions and parameters, the three-dimensional predictions show a dependence on both the generated structure and the cell number in the *third* dimension. The three-dimensional predictions increase with the *third* dimension cell number by an exponential relationship. The cell number in the *third* dimension has to be greater than a certain value to eliminate the influence and the predicted effective thermal conductivity then becomes independent of the cell number in the *third* dimension.

For given porosities, the two-dimensional predicted effective thermal conductivity is always smaller than the three-dimensional result unless the porosity equals zero or unity. The ratio of the two reaches a minimum value at a certain porosity level. Comparisons between the numerical predictions and the experimental data show that the hot-probe and hot-wire based methods are two-dimensional measurement techniques, whereas the transient comparative method is more applicable to three-dimensional situations. The methods and analyses presented in this work can be generalized for various heterogeneous materials.

Acknowledgments

The present work is supported by the National Textile Center (NTC) M04-CD01. The authors would also like to acknowledge the helpful discussions with Dr J F Zhang and Dr J K Carson.

References

[1] Muskat M and Wyckoff R D 1937 *The Flow Of Homogeneous Fluids Through Porous Media* (New York: McGraw-Hill)
[2] Ghildyal B P and Tripathi R P 1973 *Soil Physics* (London: Wiley)
[3] Zimmerman R W 1991 *Compressibility of Sandstones* (New York: Elsevier)
[4] Ingham D B, Bejan A, Mamut E and Pop I 2003 *Emerging Technologies and Techniques in Porous Media* (London: Kluwer)
[5] Sayari A and Jaroniec M 2005 *Nanoporous Materials IV* (New York: Elsevier)
[6] Ingham D B and Pop I 2005 *Transport Phenomena in Porous media III* (Oxford: Elsevier)
[7] Pan N and Zhong W 2006 *Fluid Transport Phenomena in Fibrous Materials* (Cambridge, UK: Woodhead Publishing)
[8] Blackwell J H 1954 A Transient-flow method for determination for thermal constants of insulating materials in bulk *J. Appl. Phys.* **25** 137–44
[9] Blackwell J H 1956 The axial-flow error in the thermal-conductivity probe *Can. J. Phys.* **34** 412–17
[10] Carslaw H S and Jaeger J C 1959 *Conduction of Heat in Solids* (Oxford: Clarendon)
[11] Sepaskhah A R and Boersma L 1979 Thermal-conductivity of soils as a function of temperature and water-content *Soil Sci. Soc. Am. J.* **43** 439–44
[12] Singh A K, Singh R, Chaudhary D R 1990 Prediction of effective thermal conductivity of moist porous materials *J. Phys. D: Appl. Phys.* **23** 698–702
[13] Liang X G, Ge X S, Zhang Y P, Wang G J A 1991 convenient method of measuring the thermal-conductivity of biological tissue *Phys. Med. Biol.* **36** 1599–605
[14] Liang X G 1995 The boundary induced error on the measurement of thermal-conductivity by transient hot-wire method *Meas. Sci. Technol.* **6** 467–71

[15] Liang X G, Zhang Y P and Ge X S 1999 The measurement of thermal conductivities of solid fruits and vegetables *Meas. Sci. Technol.* **10** N82–6

[16] Zhang H F, He L Q, Cheng S X, Zhai Z T and Gao D Y 2003 A dual-thermistor probe for absolute measurement of thermal diffusivity and thermal conductivity by the heat pulse method *Meas. Sci. Technol.* **14** 1396–401

[17] Zhang H F, Zhao G, Ye H, Ge X S and Cheng S X 2005 An improved hot probe for measuring thermal conductivity of liquids *Meas. Sci. Technol.* **16** 1430–5

[18] Rahman S 1995 *Food Properties Handbook* (Boca Raton, Fl: CRC Press)

[19] Liang X G and Qu W L 1997 An improved single-plate method for measuring the thermal resistance of fibrous materials *Meas. Sci. Technol.* **8** 525–9

[20] Calmidi V V and Mahajan R L 1999 The effective thermal conductivity of high porosity fibrous metal foams *J. Heat Transfer ASME* **121** 466–71

[21] Paek J W, Kang B H, Kim S Y and Hyun J M 2000 Effective thermal conductivity and permeability of aluminum foam materials *Int. J. Thermophys.* **21** 453–64

[22] Bhattacharya A, Calmidi V V and Mahajan R L 2002 Thermophysical properties of high porosity metal foams *Int. J. Heat Mass Transfer* **45** 1017–31

[23] Carson J K, Lovatt S J, Tanner D J and Cleland A C 2004 Experimental measurements of the effective thermal conductivity of a pseudo-porous food analogue over a range of porosities and mean pore sizes *J. Food Eng.* **63** 87–95

[24] Bouguera A 1999 Prediction of effective thermal conductivity of moist wood concrete *J. Phys. D: Appl. Phys.* **32** 1407–14

[25] Liang X G and Qu W 1999 Effective thermal conductivity of gas-solid composite materials and the temperature difference effect at high temperature *Int. J. Heat Mass Transfer.* **42** 1885–93

[26] Staggs J E J 2002 Estimating the thermal conductivity of chars and porous residues using thermal resistor networks *Fire Safety J.* **37** 107–19

[27] Singh R and Kasana H S 2004 Computational aspects of effective thermal conductivity of highly porous metal foams *Appl. Therm. Eng.* **24** 1841–9

[28] Ma Y T, Yu B M, Zhang D M and Zou M Q 2004 Fractal geometry model for effective thermal conductivity of three-phase porous media *J. Appl. Phys.* **95** 6426–34

[29] Carson J K, Lovatt S J, Tanner D J and Cleland A C 2006 Predicting the effective thermal conductivity of unfrozen, porous foods *J. Food Eng.* **75** 297–307

[30] Wang J F, Carson J K, North M F and Cleland D J 2006 A new approach to modeling the effective thermal conductivity of heterogeneous materials *Int. J. Heat Mass Transfer* **49** 3075–83

[31] Thovert J F, Wary F and Adler P M 1990 Thermal conductivity of random media and regular fractals *J. Appl. Phys.* **68** 3872–83

[32] Bakker K 1997 Using the finite element method to compute the influence of complex porosity and inclusion structures on the thermal and electrical conductivity *Int. J. Heat Mass Transfer* **40** 3503–11

[33] Zhang D X 2002 *Stochastic Method for Flow in Porous Media* (London: Academic)

[34] Kulasiri D and Verwoerd W 2002 *Stochastic Dynamics Modeling Solute Transport in Porous Media* (New York: Elsevier)

[35] Shoshany Y, Prialnik D and Podolak M 2002 Monte Carlo Modeling of the thermal conductivity of porous cometary ice *Icarus* **157** 219–27

[36] Barta S and Dieska P 2002 Effective thermal conductivity of particulate composite materials *Kovove Materialy-Metallic Materials* **40** 99–112

[37] Zhang H F, Ge X S and Ye H 2005 Effectiveness of the heat conduction reinforcement of particle filled composites *Modelling Simul. Mater. Sci. Eng.* **13** 401–12

[38] Zhang H F, Ge X S and Ye H 2006 Randomly mixed model for predicting the effective thermal conductivity of moist porous media *J. Phys. D: Appl. Phys.* **39** 220–26

[39] Qian J Y, Li Q, Yu K and Xuan Y M 2004 A novel method to determine the effective thermal conductivity of porous materials *Sci. China, Ser.* E **47** 716–24

[40] Wang M, Wang J K, Pan N and Chen S Y 2007 Mesoscopic predictions of the effective thermal conductivity of microscale random porous media *Phys. Rev.* E at press

[41] Wang J K, Wang M and Li Z X 2006 A lattice boltzmann algorithm for fluid-solid conjugate heat transfer *Int. J. Thermal Sci.* at press (doi: 10.1016/j.thermalsci.2006.04.012)

[42] Chen S Y and Doolen G D 1998 Lattice Boltzmann method for fluid flows *Annu. Rev. Fluid Mech.* **30** 329–64

[43] Raabe D 2004 Overview of the lattice Boltzmann method for nano- and micorscale flow dynamics in materials science and engineering *Modelling Simul. Mater. Sci. Eng.* **12** R13–46

[44] Wang J K, Wang M and Li Z X 2006 Lattice Poisson–Boltzmann simulations of electro-osmotic flows in microchannels *J. Colloid Interface Sci.* **296** 729–36

[45] Raabe D 2004 Overview of the lattice Boltzmann method for nano- and micorscale flow dynamics in materials science and engineering *Modelling Simul. Mater. Sci. Eng.* **12** R13–46

[46] Kang Q J, Zhang D X, Lichtner P C and Tsimpanogiannis I N 2004 Lattice Boltzmann model for crystal growth from supersaturated solution *Geophys. Res. Lett.* **31** L21604

[47] Doolen G D 1990 *Lattice Gas Methods for Partial Differential Equations* (New York: Addison Wesley)

[48] Succi S 2001 *The Lattice Boltzmann Equation for Fluid Dynamics and Beyond* (London: Oxford Science Press)

[49] He X Y, Chen S Y and Doolen G D 1998 A novel thermal model for the lattice Boltzmann method in incompressible limit *J. Comput. Phys.* **146** 282–300

[50] Peng Y, Shu C and Chew Y T 2003 Simplified thermal lattice Boltzmann model for incompressible thermal flows *Phys. Rev.* E **68** 026701

[51] Peng Y, Shu C and Chew Y T 2003 A 3D incompressible thermal lattice Boltzmann model and its application to simulate natural convection in a cubic cavity *J. Comput. Phys.* **193** 260–74

[52] D'Orazio A and Succi S 2003 Boundary conditions for thermal lattice Boltzmann simulations *Lect. Notes Comput. Sci.* **2657** 977–86

[53] Zou Q S and He X Y 1997 On pressure and velocity boundary conditions for the lattice Boltzmann BGK model *Phys. Fluids* **9** 1591–8

[54] Coveney P V, Maillet J B, Wilson J L, Fowler P W, Al-Mushadani O and Boghosian B M 1998 Lattice-gas simulations of ternary amphiphilic fluid flow in porous media *Int. J. Modern Phys.* C **9** 1479–90

[55] Meakin P 1998 *Fractals, Scaling and Growth Far from Equilibrium* (Cambridge: Cambridge University Press)

[56] Wang M and Li Z X 2004 Numerical simulations on performance of MEMS-based nozzles at moderate or low temperatures *Microfluidics and Nanofluidics* **1** 62–70

[57] Guo Z Y and Li Z X 2003 Size effect on single-phase channel flow and heat transfer at microscale *Int. J. Heat Fluid Flow* **24** 284–98

[58] Wang M and Li Z X 2004 Three-dimensional effect of gas flow in micro channels *J. Eng. Thermophys.* **25** 840–2

[59] Kirkpatrick S 1973 Percolation and Conduction *Rev. Mod. Phys.* **45** 574–88

[60] Li D Y 2006 Personal Communications, Department of Mechanical Engineering, Vanderbilt University

[61] Fukusako S 1990 Thermophysical properties of ice, snow and sea ice *Int. J. Thermophys.* **11** 353–72

[62] Carson J K, Lovatt S J, Tanner D J and Cleland A C 2005 Thermal conductivity bounds for isotropic, porous materials *Int. J. Heat and Mass Transfer* **48** 2150–8